

RESEARCH

Open Access



Quantitative phosphoproteomics reveals that nestin is a downstream target of dual leucine zipper kinase during retinoic acid-induced neuronal differentiation of Neuro-2a cells

Guillaume St-Cyr¹, Daniel Garneau¹, Nicolas Gévry¹ and Richard Blouin^{1*}

Abstract

Background Dual leucine zipper kinase (DLK) is critical for neurite outgrowth in the developing nervous system and during nerve regeneration, but the underlying mechanisms remain largely unknown. To address this issue, we generated stable shRNA-mediated DLK-depleted Neuro-2a cell lines and analyzed their phosphoproteome after induction of neuronal differentiation by retinoic acid (RA).

Results Here, we report the identification of 32 phosphopeptides that exhibited significant differences in relative abundance between control and DLK-depleted cells. Two of the most downregulated phosphopeptides identified after DLK depletion were derived from nestin, a type VI intermediate filament (IF) protein typically expressed in neural progenitor cells. The reduced abundance of these phosphopeptides in response to DLK knockdown was validated using parallel reaction monitoring (PRM)-based quantitative proteomics and paired with a concomitant reduction in nestin mRNA and protein expression, indicating that the decrease in nestin phosphorylation was due to a decrease in total nestin in DLK-depleted cells compared to control cells. This DLK-mediated regulation of nestin expression had no apparent effect on neurite formation because nestin knockdown alone was not sufficient to impair RA-induced neurite extension in parental Neuro-2a cells, and nestin overexpression failed to rescue the neurite outgrowth defect observed in DLK-depleted Neuro-2a cells.

Conclusions Together, these results demonstrate that nestin is a novel downstream target of DLK signaling but not a mediator of its ability to promote neurite outgrowth during neuronal differentiation.

Keywords DLK, Nestin, Neuronal differentiation, Neurite outgrowth, Neuro-2a neuroblastoma cells

*Correspondence:

Richard Blouin

Richard.Blouin@USherbrooke.ca

¹Département de biologie, Faculté des sciences, Université de Sherbrooke, Sherbrooke, Québec, Canada



© The Author(s) 2025. **Open Access** This article is licensed under a Creative Commons Attribution-NonCommercial-NoDerivatives 4.0 International License, which permits any non-commercial use, sharing, distribution and reproduction in any medium or format, as long as you give appropriate credit to the original author(s) and the source, provide a link to the Creative Commons licence, and indicate if you modified the licensed material. You do not have permission under this licence to share adapted material derived from this article or parts of it. The images or other third party material in this article are included in the article's Creative Commons licence, unless indicated otherwise in a credit line to the material. If material is not included in the article's Creative Commons licence and your intended use is not permitted by statutory regulation or exceeds the permitted use, you will need to obtain permission directly from the copyright holder. To view a copy of this licence, visit <http://creativecommons.org/licenses/by-nc-nd/4.0/>.

Background

Neuronal differentiation is fundamental to the development and regeneration of the nervous system. During this process, newborn neurons cease proliferating and undergo profound morphological changes, which result first in the formation of neurites at the cell surface. Subsequently, these neurites elongate and branch to form axons and dendrites in mature neurons, promoting the assembly of functional neuronal circuits. In keeping with its complexity, neurite outgrowth is controlled by a large number of cell-extrinsic and cell-intrinsic factors. Prominent among these are neurotrophic factors, retinoids, extracellular matrix (ECM)-associated proteins, cell adhesion molecules (CAMs), intracellular protein kinases, small GTPases, cytoskeletal components and transcription factors [1–3].

Dual leucine zipper kinase (DLK) is an attractive candidate regulator of neuronal process outgrowth and maintenance due to its divergent functional properties. This protein acts as a component of the c-Jun N-terminal kinase (JNK) pathway [4], which, in addition to its role in the transduction of signals from cytokines, growth factors and environmental stress, contributes to brain development and synaptic plasticity [5]. Depending on the origin of the neurons, developmental stage and physiological context [6], it has been reported that DLK can stimulate axon growth and regeneration as well as axon degeneration and neuronal cell death. Clues regarding the involvement of DLK in the positive regulation of neurite and axon formation are derived from studies showing that inactivation of the murine DLK gene results in abnormal brain development characterized by defects in axon growth and neuronal migration [7]. Consistent with this finding, the loss of DLK was shown to impair axonal growth in optic and sciatic nerve crush injury mouse models [8, 9], suggesting that DLK is required for axon regeneration in the peripheral nervous system (PNS). Furthermore, DLK was identified as an essential mediator of the pro-regenerative effects of cAMP on axon growth in mouse dorsal root ganglion (DRG) neurons [10]. In addition to the abovementioned reports, genetic deletion of DLK in non-regenerating central nervous system (CNS) neurons significantly attenuated axonal degeneration and neuronal cell death caused by mechanical injury and glutamate-induced excitotoxicity [9, 11–13] or observed in mouse models of amyotrophic lateral sclerosis and Alzheimer's disease [14]. Taken together, these data suggest that, in addition to its role in neural development, DLK acts as a sensor of axonal injury in neurons of the PNS and CNS to mediate axonal regeneration and degeneration, respectively.

From a mechanistic point of view, little is currently known about how DLK regulates neurite and axon outgrowth. One of the mechanisms potentially contributing

to this response is the perturbation of microtubule dynamics since the loss of DLK in mice results in reduced phosphorylation of the microtubule-stabilizing proteins doublecortin, MAP2c and MAP1B [7, 15], which are known to be involved in neurite outgrowth [16–18]. Knockout studies in mice have also shown that the absence of DLK impairs the injury-induced axonal retrograde transport of phosphorylated c-Jun and STAT3 [8], two transcription factors that promote axonal regeneration in the PNS [19, 20]. Another clue about the mechanisms involved in the regulatory effect of DLK on axonal growth comes from the observation that DLK signaling in differentiated mouse neuroblastoma Neuro-2a cells regulates the expression of many genes known for their roles in neurite formation and axon guidance, including neuropilin 1 and plexin A4 [21].

To further explore how DLK regulates neurite and axon outgrowth, we investigated the effect of DLK loss on the phosphoproteome of retinoic acid (RA)-differentiated Neuro-2a cells using an isobaric tags for relative and absolute quantitation (iTRAQ) proteomics strategy. This approach allowed us to identify 32 phosphopeptides, representing 27 phosphoproteins whose abundance was significantly altered in DLK-depleted cells exposed to RA compared to that in control cells. Among these phosphoproteins, we focused our attention on the intermediate filament (IF) protein nestin [22, 23], a neural stem/progenitor cell marker not known to be involved in DLK signaling, and its connection to neuritogenesis.

Methods

Cell culture and treatment

Mouse Neuro-2a neuroblastoma cells (ATCC[®] CCL-131[™]) were purchased from the American Type Culture Collection (Rockville, MD, USA) and grown in Dulbecco's modified Eagle's medium (DMEM) (Wisent Inc., Saint-Jean-Baptiste, Quebec, Canada) supplemented with 10% (v/v) Gibco fetal bovine serum (FBS) (Thermo Fisher Scientific Inc., Waltham, MA, USA), 100 U/ml penicillin (Wisent Inc., Saint-Jean-Baptiste, Quebec, Canada) and 100 µg/ml streptomycin (Wisent Inc., Saint-Jean-Baptiste, Quebec, Canada). When indicated, the cells were differentiated by incubating them in DMEM supplemented with 2% bovine serum albumin (BSA) and 20 µM retinoic acid (Sigma-Aldrich Canada Ltd., Oakville, Ontario) solubilized in dimethyl sulfoxide (DMSO, Sigma-Aldrich Canada Ltd., Oakville, Ontario) for 24 h or more.

Lentivirus production and generation of stable Neuro-2a cell lines

HEK293T cells (ATCC[®] CRL-11268[™]) were purchased from the American Type Culture Collection (Rockville, MD, USA) and grown in DMEM supplemented with

10% (v/v) FBS and antibiotics. For lentivirus production, cells were cotransfected with the envelope protein-expressing vector pMD2. G and the packaging protein expression vector psPAX2 (kindly provided by Dr. Didier Trono University of Geneva Medical School, Geneva, Switzerland) and with either the empty lentiviral vector pLKO.1 [24] (plasmid 8453, Addgene, Cambridge, MA, USA) or the pLKO.1-based lentiviral mouse DLK shRNA vector (clone TRCN0000022569 [shDLK#1] or clone TRCN0000022573 [shDLK#2], Open Biosystems, Huntsville, AL, USA) using polyethylenimine hydrochloride (#24765, PEI MAX, Polysciences, Inc., Warrington, PA, USA) at a ratio of 1 µg:3 µl. At 72 h posttransfection, the culture medium containing the lentiviruses was harvested, filtered through a 0.45-µm filter, and used for infection. Neuro-2a cells were seeded at a density of 2.0×10^6 cells in 100-mm dishes 24 h before infection with viral supernatants supplemented with 8 µg/ml polybrene (Sigma-Aldrich Canada Ltd., Oakville, Ontario). Two days later, the infected cells were treated with puromycin (2 µg/ml, Sigma-Aldrich Canada Ltd., Oakville, Ontario) and selected for several days until a stable pool of resistant cells was obtained.

Cell lysate preparation and immunoblotting

Preparation of cell lysates, SDS-PAGE and immunoblotting were carried out as described previously [25]. When indicated, cytoskeletal proteins were prepared from cultured cells according to the procedure of Choi et al. [26] and subsequently processed for immunoblotting analysis using either an anti-nestin or anti-vimentin antibody. Immunoreactive bands were detected by enhanced chemiluminescence (Western Lightning Plus-ECL, PerkinElmer, Inc., Waltham, MA, USA) and quantified using a Bio-Rad ChemiDoc imaging system. β -actin or vimentin levels were used for normalization. A list of all primary and secondary antibodies used in this study is available in Supplementary File 5.

Neurite outgrowth analysis

Neurite outgrowth was quantified using the NeuroTrack software module of the IncuCyte® S3 Live-Cell Analysis System (Essen BioScience, Inc., Ann Arbor, MI, USA) on images taken every 4 h with a 10x objective. *The segmentation mode* was set at [Texture], *the min cell width (µm)* was set at [18,000], and *the neurite sensitivity* was set at [0,4]. Measurements were conducted on twelve images (4 images, 3 wells) for each replicate of a given condition. Each experiment was performed at least in triplicate, and the resulting data were subjected to multiple unpaired *t* tests for statistical analysis.

Quantitative phosphoproteomics

Control (pLKO.1) and shDLK#2-depleted Neuro-2a cells were incubated under differentiating conditions for 24 h as described above, pelleted and then flash-frozen at -80 °C. Samples were submitted to the Proteomics Platform at the CHU de Québec Research Centre for protein extraction, trypsin digestion, peptide labeling with iTRAQ multiplex reagents (SCIEX, Concord, Ontario, Canada) and mass spectrometry (MS) analyses, as previously described [27]. In brief, proteins were extracted in lysis buffer (50 mM ammonium bicarbonate, 0.5% sodium deoxycholate, 50 mM dithiothreitol) containing protease inhibitors (Sigma-Aldrich Canada Ltd., Oakville, Ontario), a PhosSTOP phosphatase inhibitor mixture (Roche Diagnostics, Laval, Quebec) and 1 mM pepstatin. After quantification, 100 mg of protein per condition from two biological replicates was digested overnight with trypsin, followed by labeling with the iTRAQ reagent tags 114, 115, 116 and 117 for 2 h at room temperature in the dark, as suggested by the manufacturer. The labeled peptides were subsequently combined in one tube, cleaned using an HLB cartridge (Waters, Mississauga, Ontario, Canada), subjected to phosphopeptide enrichment on TiO_2 beads and purified on a graphite column (#A32993, High-Select™ TiO_2 Phosphopeptide Enrichment Kit, Thermo Fisher Scientific, Waltham, MA, USA). The phosphopeptide sample was analyzed by nanoLC-MS/MS using a Dionex Ultimate 3000 (RSLCnano) chromatography system (Thermo Fisher Scientific, Waltham, MA, USA) coupled to an Orbitrap Fusion mass spectrometer (Thermo Fisher Scientific, Waltham, MA, USA) as described previously [28]. The mass spectrometry raw files were processed and quantified using Proteome Discoverer 2.1 software (Thermo Fisher Scientific, Waltham, MA, USA) and searched against the UniProt *Mus musculus* protein database (58,654 entries) using both the Mascot and Sequest algorithms. The identified peptides and proteins were filtered at a false discovery rate of 1% using the target-decoy strategy. Only proteins identified with at least two unique peptides were considered for quantification. Normalization of the MS data and peptide ratio calculations were performed with Proteome Discoverer software. The statistical significance of differences between samples was evaluated using one-way ANOVA and z score calculations. Phosphopeptides with a p value < 0.05 and a z score > 2 were considered differentially expressed.

Parallel reaction monitoring (PRM) analysis

The levels of phosphorylated nestin at Ser-894 and Ser-137 and phosphorylated c-Jun at Ser-63 and Ser-73 were monitored in control and DLK-depleted cells from three independent experiments using PRM, an MS/MS-based method for targeted quantitation [29]. The

phosphopeptide abundance was normalized to that of cytochrome c peptides previously spiked into the samples, and subsequent quantification was performed using the Skyline software package [30]. For comparisons of data between experiments and between samples, statistical analysis was performed using an unpaired two-tailed *t* test.

RT-qPCR experiments

Total RNA was extracted with a Direct-zol RNA Mini-Prep Kit (#R2050, Zymo Research, Irvine, CA, USA) in combination with TRIzol (#15596026, Life Technologies, Burlington, Ontario, Canada) following the manufacturer's protocol. A 30 min on-column DNase treatment was performed before elution according to the manufacturer's instructions. RNA was quantified on a NanoDrop spectrophotometer (Thermo Fisher Scientific, Waltham, MA, USA). Total RNA quality was assessed with an Agilent 2100 Bioanalyzer (Agilent, Santa Clara, CA, USA). Reverse transcription was performed on 2.2 µg of total RNA with Transcriptor reverse transcriptase, random hexamers, dNTPs (Roche Diagnostics, Laval, Quebec, Canada), and 10 units of RNaseOUT (Invitrogen, Thermo Fisher Scientific, Waltham, MA, USA) following the manufacturer's protocol in a total volume of 20 µl. All forward and reverse primers were individually resuspended in 20–100 µM stock solution in Tris-EDTA buffer (Integrated DNA Technologies, Coralville, IA, USA) and diluted to 1 µM in RNase DNase-free water (Integrated DNA Technologies, Coralville, IA, USA). qPCR was performed in 10 µl in 96-well plates on a CFX96 thermocycler (Bio-Rad Laboratories, Mississauga, Ontario, Canada) with 5 µl of 2X iTaq Universal SYBR Green Supermix (Bio-Rad Laboratories, Mississauga, Ontario, Canada), 10 ng (3 µl) cDNA, and 200 nM final (2 µl) primer pair solution. The following cycling procedure was used: 3 min at 95 °C; 50 cycles of 15 s at 95 °C, 30 s at 60 °C, and 30 s at 72 °C. Relative expression levels were calculated using the qBASE framework [31] and the housekeeping genes *Psmc4*, *Pum1* and *Txn14b* for mouse cDNA. Primer design and validation were evaluated as described elsewhere [32]. In every qPCR run, a no-template control was performed for each primer pair, and the results were consistently negative. All primer sequences are available in Supplementary File 6.

Plasmids and transfection

The expression plasmid for wild-type mouse nestin (#MC202576) was obtained from OriGene (Rockville, MD, USA). Transient transfection of Neuro-2a cells was carried out by using 1 µg of the nestin expression vector per ml of growth medium and PEI MAX (Polysciences Inc. Warrington, PA, USA). Cells were harvested and processed for Western blotting 48 h after transfection.

RNA interference

RNA interference was achieved transiently using small interfering RNA (siRNA) targeting murine nestin (siGENOME set of four, #MQ-057300-01-0002 [D-057300-01, D-057300-03, D-057300-04, D-057300-17]; Dharmacon, Lafayette, CO, USA); nontargeting control siRNAs (ON-TARGETplus Nontargeting Control Pool, #D0018101005, Dharmacon, Lafayette, CO, USA); and Lipofectamine® RNAiMAX transfection reagent (#13778100, Thermo Fisher Scientific, Waltham, MA, USA). The assays were performed as suggested by *Lipofectamine® RNAiMAX Reagent Protocol 2013*. Neuro-2a cells were seeded at a concentration of 5.0×10^3 cells per well in a 96-well plate.

Statistical analysis

Statistical significance of immunoblot and RT-qPCR data was determined by unpaired two-tailed Student's *t* test and expressed as the means ± SEMs. Comparisons of neurite outgrowth rates between two cell groups were made using multiple unpaired *t* tests. All the statistical analyses and calculations were performed with GraphPad Prism 10 (GraphPad Software, San Diego, CA, USA). A *p* value of < 0.05 was considered statistically significant.

Results

Generation and characterization of a Neuro-2a cell model to investigate the molecular mechanisms of DLK-mediated neurite outgrowth

DLK has been recognized as a key regulator of nervous system development and regeneration due to its ability to modulate axon growth [7, 11, 33]. Consistent with this, we previously used the established mouse neural crest-derived cell line Neuro-2a to show that transient depletion of DLK results in the inhibition of neurite outgrowth [21]. To further investigate how DLK contributes to neurite outgrowth, we first generated stable Neuro-2a cell lines in which DLK expression was downregulated by RNA interference. Neuro-2a cells were infected with lentiviral vectors expressing two different short hairpin RNAs (shRNAs) that target mouse DLK mRNA (shDLK#1 and shDLK#2), followed by selection with puromycin for several days and expansion. As a negative control, cells were also infected with an empty lentiviral vector (pLKO.1). Knockdown of DLK expression in cells grown in proliferating (DMEM with 10% FBS) or differentiating (DMEM with 2% FBS + 20 µM retinoic acid (RA)) media for 24 h was confirmed by immunoblot analysis. As shown in Fig. 1A and B, compared with that in control cells, DLK protein expression in cells infected with the shDLK#1 and shDLK#2 constructs was reduced by approximately 50% and 75%, respectively. Parallel immunoblot analyses using antibodies specific for the phosphorylated, activated forms of JNK and c-Jun, two downstream targets of DLK, revealed that DLK depletion significantly

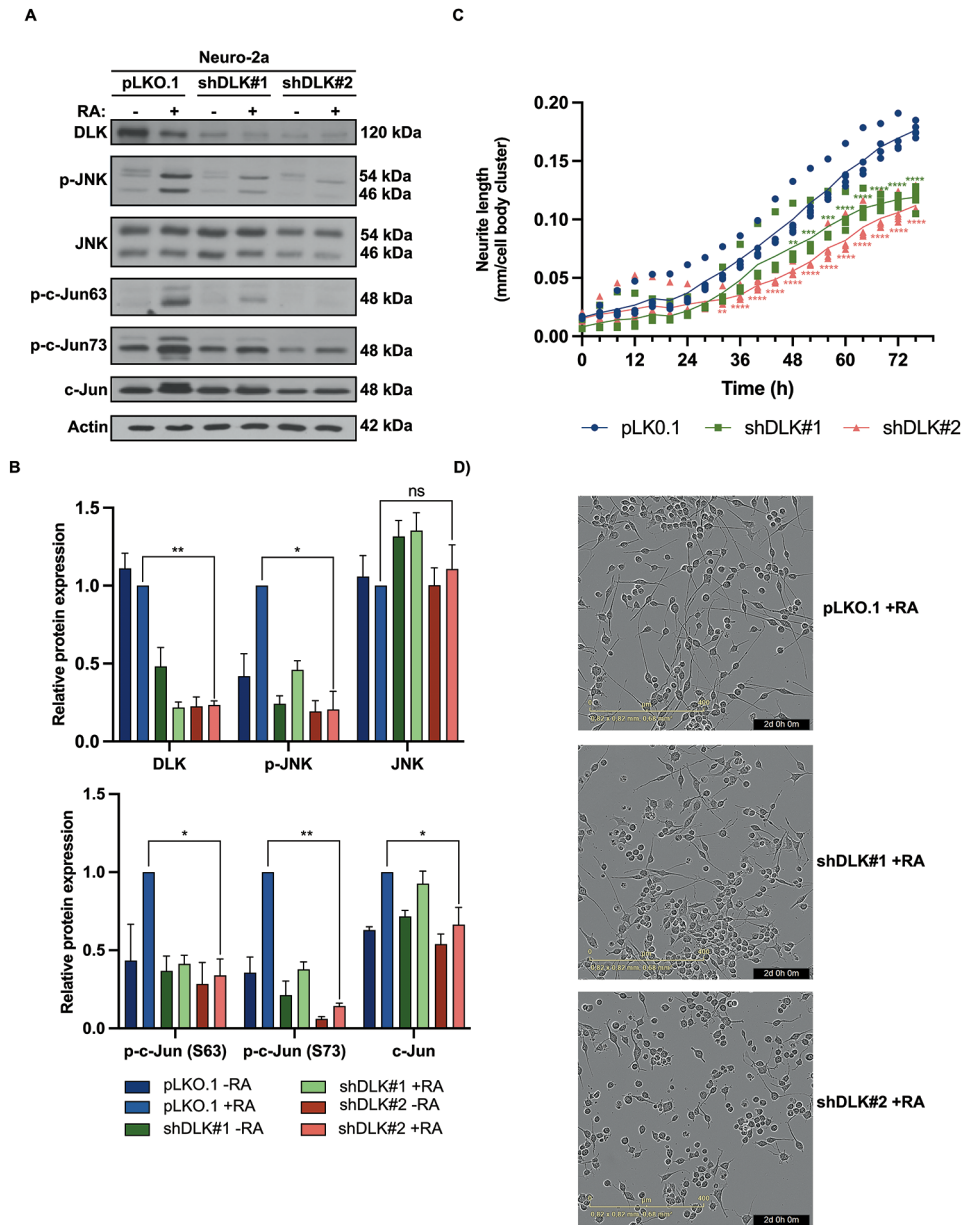


Fig. 1 Knockdown of DLK in Neuro-2a cells. Neuro-2a cells were infected with an empty lentiviral vector (pLKO.1) or with lentivirus expressing mouse DLK shRNAs (shDLK#1 and shDLK#2), followed by selection with puromycin to establish stable cell lines. **(A)** Representative Western blots showing the levels of DLK, phospho-JNK, total JNK, phospho-c-Jun (Ser-63 or Ser-73), c-Jun and actin in control and DLK-depleted Neuro-2a cells incubated without (-) or with (+) 20 μ M retinoic acid (RA) for 24 h. Bands of interest were excised from different blots and grouped together. Full-length blots are presented in Supplementary File 1. **(B)** Quantification of DLK, phospho-JNK, total JNK, phospho-c-jun (Ser-63 or Ser-73) and c-Jun protein levels in control and DLK-depleted cells. All chemiluminescent signals were quantified using a Bio-Rad ChemiDoc imaging system and normalized to the actin level in control cells exposed to RA. The data are presented as the means \pm SEMs (error bars) from two or three independent experiments. Each replicate has its own actin control. Statistical significance was determined using a two-tailed unpaired Student's t test. For simplicity, only the statistical analysis of the shDLK#2-depleted Neuro-2a cells treated with RA is shown. *, $p < 0,05$; **, $p < 0,01$, relative to control cells exposed to RA. ns, not significant. **(C)** Neurite length (mm) per cell-body cluster was measured every 4 h in control and DLK-depleted cells that were exposed to RA for 76 h. Data on graph represent the individual values obtained from five independent experiments at each time point with means connected. Multiple unpaired t tests were used for statistical analysis. **, $p < 0,01$; ***, $p < 0,001$; ****, $p < 0,0001$, relative to control cells. **(D)** Representative phase contrast images of control (pLKO.1) and shDLK#1- or shDLK#2-depleted Neuro-2a cells cultured with RA for 48 h. Scale bar, 400 μ m

impaired the activation of JNK and c-Jun induced by RA (Fig. 1A and B), suggesting a role for DLK in this response. Interestingly, given the demonstrated contribution of c-Jun to the regulation of its own transcription [34], we correspondingly observed a significant decrease in its abundance in DLK-depleted cells exposed to RA. Taken together, these data demonstrated that DLK is required for the activation of JNK and c-Jun during the RA-induced differentiation of Neuro-2a cells.

To determine whether DLK depletion impairs neurite outgrowth in our shDLK#1 and shDLK#2 Neuro-2a cell lines, we examined their morphological response to differentiation conditions over a 72-hour period using the IncuCyte® S3 Live-Cell Analysis System for Neuroscience and the IncuCyte® NeuroTrack software module (Fig. 1C). In contrast to those of control cells, which exhibited extensive neurite outgrowth after RA treatment, we consistently observed fewer and shorter neurites in both the shDLK#1- and shDLK#2-depleted Neuro-2a cell lines, with the latter showing a greater defect in neurite outgrowth (Fig. 1C and D). In addition to being consistent with the demonstrated role of DLK in axon formation [35] and elongation [7], these data confirm that its presence in Neuro-2a cells is critical for neuritogenesis to proceed. Because the neurite outgrowth of the shDLK#2-depleted Neuro-2a cells was significantly reduced by RA treatment, we performed the following experiments using these cells.

Quantitative phosphoproteomic analysis of DLK-depleted Neuro-2a cells undergoing RA-induced differentiation

Depletion of DLK in Neuro-2a cells alters RA-induced differentiation, as evidenced by deficient neurite outgrowth. This difference is likely due, at least in part, to the decreased phosphorylation and activity of JNK and c-Jun (Fig. 1), both of which are involved in neurite outgrowth and axonal regeneration [36–38]. Since the role of DLK in neurite formation has not been fully characterized at the molecular level, we speculated that other effector proteins are involved in this response. To identify such unknown effectors of DLK-dependent neurite outgrowth, we examined the phosphoproteomes of control (pLKO.1) and shDLK#2-depleted Neuro-2a cells treated with RA for 24 h using the workflow shown in Fig. 2A. Briefly, after protein extraction and digestion, the resulting peptides were labeled with iTRAQ reagents to quantify protein abundance, pooled in equimolar amounts, and subjected to a phosphopeptide purification step using TiO₂ particles. Enriched phosphopeptides were subsequently identified and quantified via mass spectrometry. In total, this protocol allowed us to detect and quantify 4942 phosphopeptides on 2123 unique proteins from two independent biological replicates, each with two technical replicates. A volcano plot of all phosphopeptides

quantified in our phosphoproteomic analysis is shown in Fig. 2B. Since our goal was to identify potential effectors of DLK, we focused on phosphopeptides that exhibited at least a 1.5-fold change and a p value less than 0.05 between control and DLK-depleted cells. This statistical analysis revealed that, compared with those in the control group, only 32 phosphopeptides, derived from 27 distinct phosphoproteins, were significantly affected by DLK depletion, with 23 downregulated and 9 upregulated phosphoproteins (Table 1). Gene Ontology (GO) and functional interaction analyses of the 27 phosphoproteins were performed using the Database for Annotation, Visualization and Integrated Discovery (DAVID) and Search Tool for the Retrieval of Interacting Genes/Proteins (STRING) databases, respectively. The results revealed that many of the proteins were associated with nervous system development (Table 2) and potentially connected into a network of proteins, including among others, c-Jun, neural cell adhesion molecule 1 (Ncam1) and nestin (Fig. 2C). Our phosphoproteomic screen revealed that the phosphorylation of c-Jun, a key regulator of axonal regeneration [38], at Ser63 and Ser73 was significantly decreased upon DLK depletion, further validating the immunoblot results presented above. These two serine residues are selectively phosphorylated by JNK in response to various stimuli and are involved in c-Jun transcriptional activity [39]. Ser774 of Ncam1 is another site whose phosphorylation level significantly decreased in DLK-depleted cells undergoing RA-induced differentiation compared with that in control cells. Interestingly, phosphorylation at this site has been shown to be required for activation of the cAMP response element-binding protein (CREB) transcription factor and for neurite outgrowth [40]. Finally, an important feature of our phosphoproteomic data was the substantial decrease in the abundance of two phosphopeptides, Ser-894 and Ser-1837, of nestin, an IF protein highly expressed in neural progenitor cells [22, 23]. Although these two serine residues are known to be phosphorylated in various cellular contexts [41–43], their role in nestin dynamics and/or function has not been reported.

Given the involvement of nestin in stem cell functions, including differentiation and migration [44], we decided to focus our study on evaluating the relationship between DLK and nestin in more detail. To this end, we first confirmed the validity of our phosphopeptide data in control and DLK-depleted cells by parallel reaction monitoring (PRM) mass spectrometry, a sensitive targeted proteomics method for the selective and accurate quantification of multiple proteins or peptides simultaneously [29]. As illustrated in Fig. 2D, DLK depletion led to an expected and dramatic decrease in the abundance of phosphopeptides containing Ser63 and Ser73 of c-Jun, demonstrating the efficacy of the PRM procedure. In

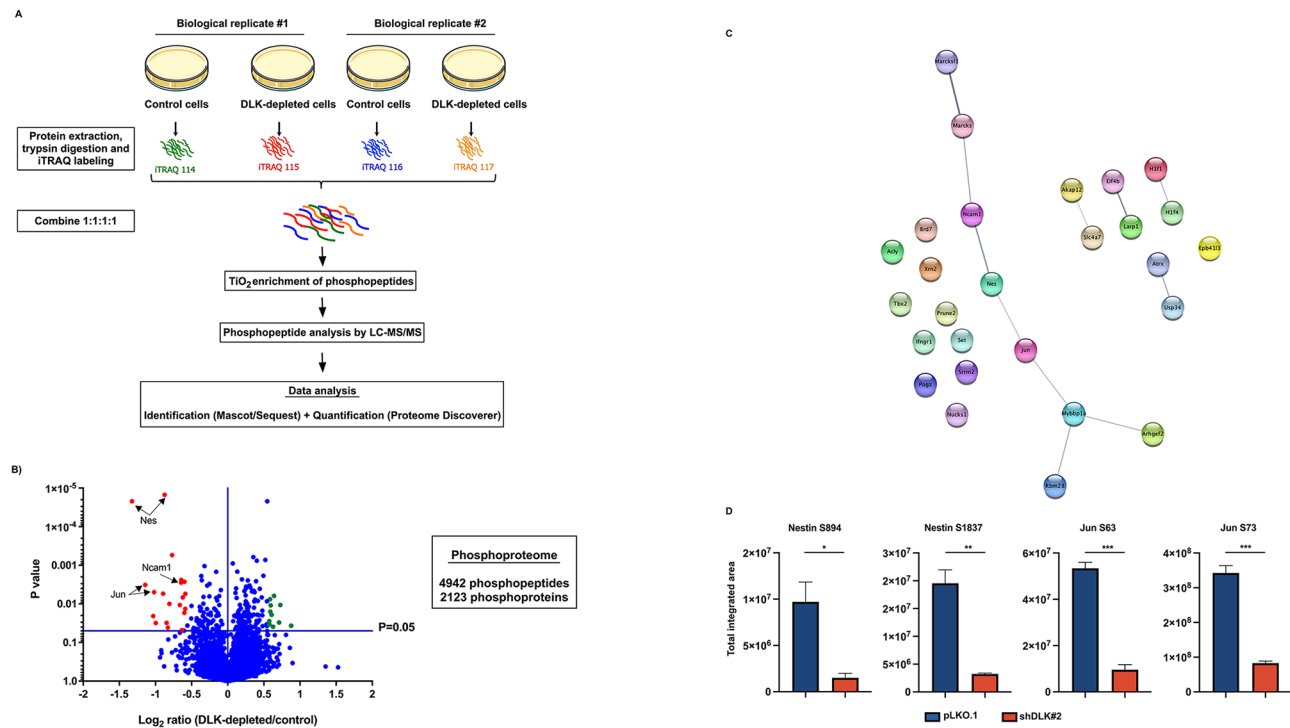


Fig. 2 Quantitative phosphoproteomic analysis of Neuro-2a cells after DLK depletion. **(A)** Scheme of the experimental procedure used to identify phosphopeptides that were either downregulated or upregulated in DLK-depleted cells after treatment with RA compared to control cells. **(B)** Volcano plot showing the \log_2 (-fold change) versus p value of all phosphopeptides (DLK-depleted/control) identified by mass spectrometry. Phosphopeptides that were downregulated or upregulated at least 1.5-fold in DLK-depleted cells are shown in red and green, respectively. **(C)** STRING interaction network of proteins exhibiting deregulated phosphorylation in DLK-depleted cells. Line thickness represents the confidence of the interaction at a medium score of 0.400. **(D)** The amount of nestin peptide with phosphorylated serine residues at positions 894 and 1837 or c-Jun with phosphorylated serine 63 and serine 73 in control and DLK-depleted cells was quantified using a PRM strategy. Integrated areas of the three major fragment ions obtained from the MS-MS spectrum of each phosphopeptide were determined, summed, and normalized to exogenous spike-in cytochrome c peptides. The data represent the mean \pm SEM of three separate experiments. Statistical significance was determined using a two-tailed unpaired Student's t test. *, $p < 0,05$; **, $p < 0,01$; ***, $p < 0,001$, relative to control cells

addition, we found that the phosphorylation levels of Ser-894 and Ser-1837 of nestin were significantly lower after DLK knockdown than after control treatment (Fig. 2D), highlighting a novel role for DLK in nestin regulation and/or function.

Changes in nestin phosphopeptide abundance after DLK depletion are associated with altered nestin mRNA and protein expression

Because the observed changes in nestin phosphopeptide abundance in DLK-depleted cells may reflect either decreased phosphorylation levels, decreased protein abundance, or both, we measured nestin mRNA and protein expression in control and DLK-depleted Neuro-2a cells that were exposed to RA for 24 h by RT-qPCR and Western blot analysis, respectively. As shown in Fig. 3A, the levels of nestin transcripts markedly increased in control cells undergoing RA-induced neuronal differentiation. In contrast, in shDLK#1- and shDLK#2-depleted cells, this increase was weaker and not significant when compared to control cells, suggesting a positive

regulatory role for DLK in the RA-induced expression of nestin. This assumption was supported by the immunoblot data obtained with cytoskeletal extracts, which showed a lack of responsiveness to RA and even a decrease in nestin abundance in DLK-depleted cells compared to control cells (Fig. 3B and C). The fact that shDLK#1 does not reduce nestin protein abundance with the same efficacy as shDLK#2 could be due to a difference in specificity between the two shRNAs and/or a difference in residual DLK levels between the two cell lines. Taken together, these results indicate that the decreased abundance of nestin phosphopeptides observed after DLK depletion was due to changes in the overall expression of nestin rather than to reduced phosphorylation.

Neither knockdown nor overexpression of nestin affects neurite outgrowth in Neuro-2a cells

In light of the results presented above, we next wondered whether the reduction of nestin levels seen in DLK-depleted cells could account for their failure to form neurites when treated with RA. To test this, we silenced

Table 2 The top 10 most enriched GO biological process terms associated with proteins exhibiting decreased or increased phosphorylation in DLK-depleted cells

Term	Count	Genes	P Value	Benjamini
Nervous system development	12	SLC4A7, JUN, MARCKSL1, MARCKS, IFNGR1, XRN2, ATRX, EPB41L3, NCAM1, ARHGEF2, NES, TBX2	1,2E-04	8,7E-02
Programmed cell death	11	AKAP12, SLC4A7, JUN, MARCKS, SET, MYBBP1A, PRUNE2, EPB41L3, NCAM1, NES, TBX2	1,3E-04	8,7E-02
Cell death	11	AKAP12, SLC4A7, JUN, MARCKS, SET, MYBBP1A, PRUNE2, EPB41L3, NCAM1, NES, TBX2	2,3E-04	8,7E-02
Positive regulation of macromolecule biosynthetic process	10	AKAP12, JUN, LARP1, MYBBP1A, POGZ, ATRX, NUCKS1, ARHGEF2, BRD7, TBX2	2,8E-04	8,7E-02
Central nervous system development	8	SLC4A7, MARCKSL1, MARCKS, IFNGR1, XRN2, ATRX, NCAM1, NES	3,0E-04	8,7E-02
Positive regulation of biosynthetic process	10	AKAP12, JUN, LARP1, MYBBP1A, POGZ, ATRX, NUCKS1, ARHGEF2, BRD7, TBX2	5,7E-04	1,4E-01
Positive regulation of nitrogen compound metabolic process	10	JUN, LARP1, MYBBP1A, IFNGR1, POGZ, ATRX, NUCKS1, ARHGEF2, BRD7, TBX2	7,3E-04	1,4E-01
Positive regulation of gene expression	10	JUN, LARP1, MYBBP1A, IFNGR1, POGZ, ATRX, NUCKS1, ARHGEF2, BRD7, TBX2	7,7E-04	1,4E-01
Camera-type eye development	5	SLC4A7, JUN, XRN2, NES, TBX2	1,2E-03	1,9E-01
Positive regulation of macromolecule metabolic process	12	AKAP12, JUN, MARCKS, LARP1, MYBBP1A, IFNGR1, POGZ, ATRX, NUCKS1, ARHGEF2, BRD7, TBX2	1,6E-03	1,9E-01

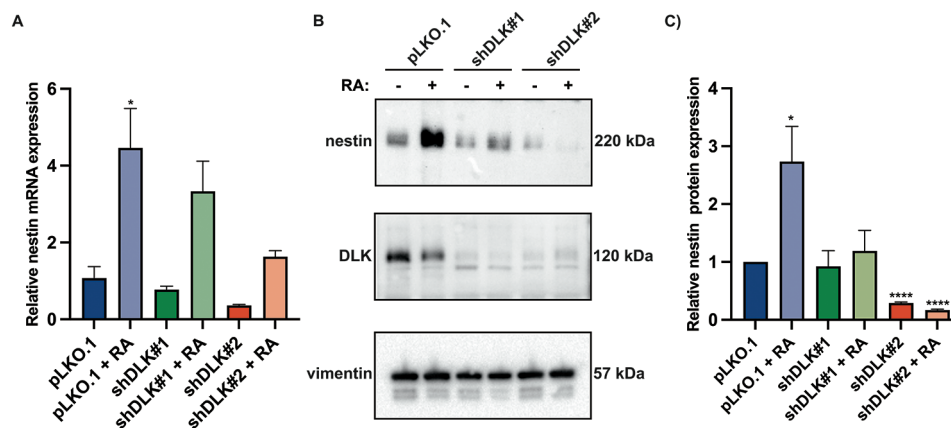


Fig. 3 Nestin expression in DLK-depleted Neuro-2a cells. **(A)** Relative level of nestin mRNA in control and DLK-depleted Neuro-2a cells incubated without or with 20 μ M RA for 24 h. The mRNA level of nestin was analyzed by quantitative RT-PCR, normalized to three housekeeping genes (Psmc4, Pum1, and Txnl4b) and calculated with the $\Delta\Delta C_T$ method. The data represent the mean \pm SEM of three separate experiments. Statistical significance was determined using a two-tailed unpaired Student's t test. *, $p < 0,05$, relative to control cells not exposed to RA. **(B)** Representative Western blots showing the levels of nestin, DLK and vimentin in control and DLK-depleted Neuro-2a cells incubated without (-) or with (+) 20 μ M RA for 24 h. Bands of interest were excised from different blots and grouped together. Full-length blots are presented in Supplementary File 2. **(C)** Quantification of nestin protein levels in control and DLK-depleted cells. Chemiluminescent signals were quantified using a Bio-Rad ChemiDoc imaging system and normalized to the vimentin level in control cells not exposed to RA. The data are presented as the means \pm SEMs (error bars) of two or three separate experiments. Each replicate has its own vimentin control. Statistical significance was determined using a two-tailed unpaired Student's t test. *, $p < 0,05$; ****, $p < 0,0001$, relative to control cells not exposed to RA

Discussion

DLK regulates nervous system development and regeneration in many model organisms, such as *Drosophila*, *C. elegans* and mice, through positive modulation of neurite outgrowth [7, 8, 33, 45]. However, exactly how DLK contributes to this process of fundamental importance in neurobiology remains a major unanswered question that we began to address in this study. Since DLK presumably exerts its function in neurite outgrowth by catalyzing the phosphorylation of specific effector proteins,

either directly or indirectly, we performed a quantitative phosphoproteomic analysis of control and DLK-depleted Neuro-2a cells undergoing RA-induced neuronal differentiation to identify such target proteins. From this experiment, we observed that, compared with the control treatment, the loss of DLK significantly up- and down-regulated the abundance of 9 and 23 phosphopeptides, respectively. Interestingly, almost half of the proteins from which the identified phosphopeptides were derived were enriched in GO biological process terms linked to

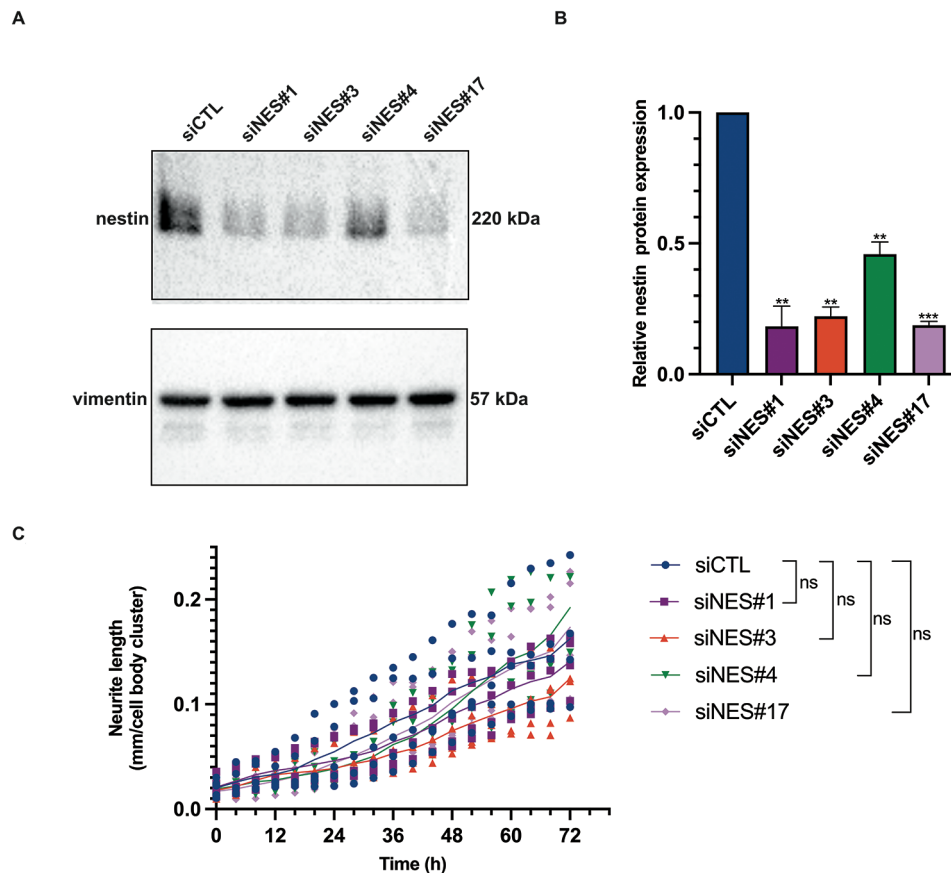


Fig. 4 Knockdown of nestin in Neuro-2a cells has no impact on RA-induced neurite outgrowth. **(A)** Neuro-2a cells grown in proliferation medium were transfected with either a nontargeting control (siCTL) or four different nestin-specific siRNAs (siNES#1, #3, #4, and #17). At 48 h after transfection, the cytoskeleton was prepared and processed for western blot analysis using antibodies against nestin and vimentin. Bands of interest were excised from different blots and grouped together. Full-length blots are presented in Supplementary File 3. **(B)** Quantification of nestin protein levels in control and nestin-depleted cells. Chemiluminescent signals were quantified using a Bio-Rad ChemiDoc imaging system and normalized to the vimentin level in control cells. The data are presented as the means \pm SEMs (error bars) of three separate experiments. Each replicate has its own vimentin control. Statistical significance was determined using a two-tailed unpaired Student's *t* test. **, $p < 0,01$; ***, $p < 0,001$. **(C)** Neurite length (mm) per cell-body cluster was measured every 4 h in control and nestin siRNA-transfected cells that were exposed to RA for 72 h. Data on graph represent the individual values obtained from five independent experiments at each time point with means connected. Multiple unpaired *t* tests were used for statistical analysis. ns, not significant compared with the control cells

nervous system development and included proteins with a predicted functional relationship, such as Jun, Nes, Ncam1, Marcks and Marcksl1. Among this list of candidate proteins, we decided to focus on nestin for two particular reasons: first, it exhibited the most dramatic reduction in phosphopeptide abundance in DLK-knockdown cells; second, previous studies have provided some evidence supporting its relevance to the differentiation and migration of stem cells, particularly those of the neural lineage [46]. However, using RT-qPCR and Western blotting, we were able to show that the observed decrease in nestin phosphorylation following DLK depletion correlated with reduced nestin expression at both the mRNA and protein levels, suggesting a possible role for DLK in the regulation of overall nestin abundance rather than phosphorylation.

Although nestin was identified more than 30 years ago [47], very little is known about its regulation and function. The mammalian nestin gene consists of four exons and three introns [48–50]. An enhancer element residing within the second intron regulates nestin expression in the developing central nervous system (CNS) and during RA-induced neural differentiation of P19 embryonic carcinoma cells [51]. This enhancer contains various types of cis-acting elements, such as hormone-response elements (HREs) and binding sites for the Sox and POU transcription factors, which orchestrate nestin gene expression in neural stem/progenitor cells (NSPCs) both in vitro and in vivo. Interestingly, Sox transcription factors are highly relevant for the development of the nervous system, and three of them, namely Sox1, Sox2 and Sox3, are differentially expressed in NT2/D1 cells undergoing neural differentiation with RA [52]. Histone acetylation,

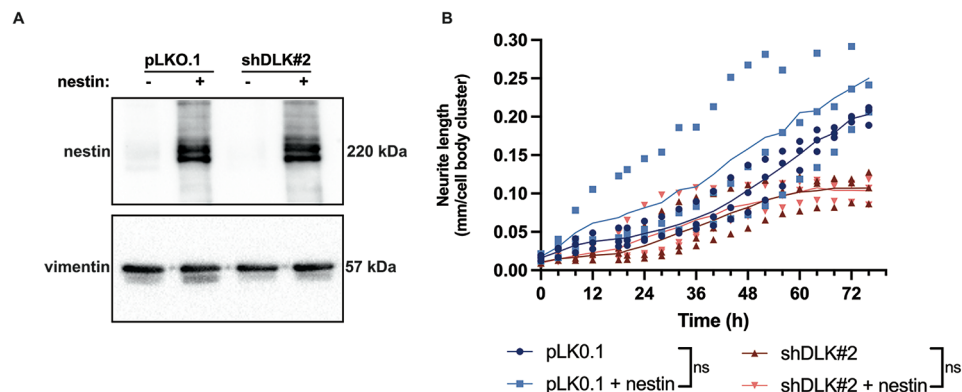


Fig. 5 Overexpression of nestin does not rescue the neurite outgrowth defect in DLK-depleted cells. **(A)** Control (pLKO.1) and shDLK#2/DLK-depleted Neuro-2a cells were transfected with plasmids expressing either EGFP (control) or wild-type nestin and grown in proliferation medium. At 48 h after transfection, the cytoskeleton was prepared and processed for western blot analysis using antibodies against nestin and vimentin. Bands of interest were excised from different blots and grouped together. Full-length blots are presented in Supplementary File 4. **(B)** Neurite length (mm) per cell-body cluster was measured every 4 h in control and shDLK#2/DLK-depleted cells that were differentiated from RA for 76 h two days after transfection with EGFP or nestin. Data on graph represent the individual values obtained from three independent experiments at each time point with means connected. Multiple unpaired *t* tests were used for statistical analysis. ns, not significant

an epigenetic mechanism, is also known to mediate the activation of nestin transcription during the differentiation of P19 cells along the neural cell lineage [53]. Consistent with what has been previously described in murine embryonic stem cells [54] and P19 cells [55], treatment with RA, a vitamin A derivative essential for brain development, neuronal differentiation and neurite outgrowth [56], significantly increased nestin expression in Neuro-2a cells (Fig. 3). Like other lipophilic hormones, the action of RA in this cell line likely by probably involves genomic and nongenomic pathways [57]. The genomic effect of RA on the expression of target genes is mediated by interactions with the nuclear receptors retinoic acid receptor (RAR) and retinoid X receptor (RXR), which function as transcription factors, while its nongenomic action involves the activation of kinase cascades, which, in turn, modulate cytoplasmic and nuclear events through the phosphorylation of specific target proteins [57, 58]. To the best of our knowledge, no studies have been performed to elucidate in detail how RA upregulates nestin expression in stem cells committed to a neuronal fate. In the present study, we found that DLK is likely an important component of the mechanism underlying RA-induced nestin expression, as its knockdown in Neuro-2a cells significantly impaired this response at both the mRNA and protein levels (Fig. 3). Since variations in mRNA levels are typically attributed to changes in synthesis (transcription) rather than degradation, it is likely that DLK depletion affects nestin gene expression in RA-treated cells by disrupting chromatin remodeling and/or the binding of transcriptional regulators. Although DLK itself is not known to directly recruit the general transcriptional machinery or initiate transcription, its effector, JNK, has this capability. Indeed, JNK

interacts with, phosphorylates, and regulates various transcription factors (e.g. c-Jun, ATF2, Sox2, STAT3, RAR α , PPAR γ , POU2F1, POU5F1) as well as chromatin-associated proteins (e.g. histone H3, bromodomain protein 4) [39, 59–64]. An effect of DLK depletion on nestin protein synthesis and/or stability is also plausible, given the results of previous work showing that: (i) DLK regulates the synthesis of Down syndrome cell adhesion molecule (Dscam) in *Drosophila* via the poly(A)-binding protein PABP-C, an activator of protein translation [65], and (ii) its effector, JNK, enhances the stability of certain proteins, such as c-Jun, via phosphorylation [66, 67]. Thus, our study identifies DLK as a downstream mediator of RA signaling that governs nestin expression during neuronal differentiation (Fig. 6). While the physiological relevance of this regulation remains unclear, it suggests a role for DLK in modulating of nestin function.

As mentioned above, nestin is an IF protein predominantly expressed in NSPCs of the nervous system [44]. Upon their differentiation and concomitant loss of multipotency, nestin expression decreases, and nestin is replaced by other IF proteins, namely, neurofilaments and glial fibrillary acidic protein, in the neuronal and glial cell lineages, respectively [49, 68]. Whether this downregulation of nestin plays an active role in the switch from growth to differentiation of neural cells has not been well studied. Mice deficient in nestin are viable and develop normally like wild-type mice but exhibit increased neurogenesis in the adult hippocampal dentate gyrus [69], suggesting a negative role for nestin in the control of this process. In support of this notion, Wilhelmsson et al. [70] also reported that dissociated neurospheres from Nes^{-/-} mice generate more neurons than do those from wild-type animals when grown under differentiation

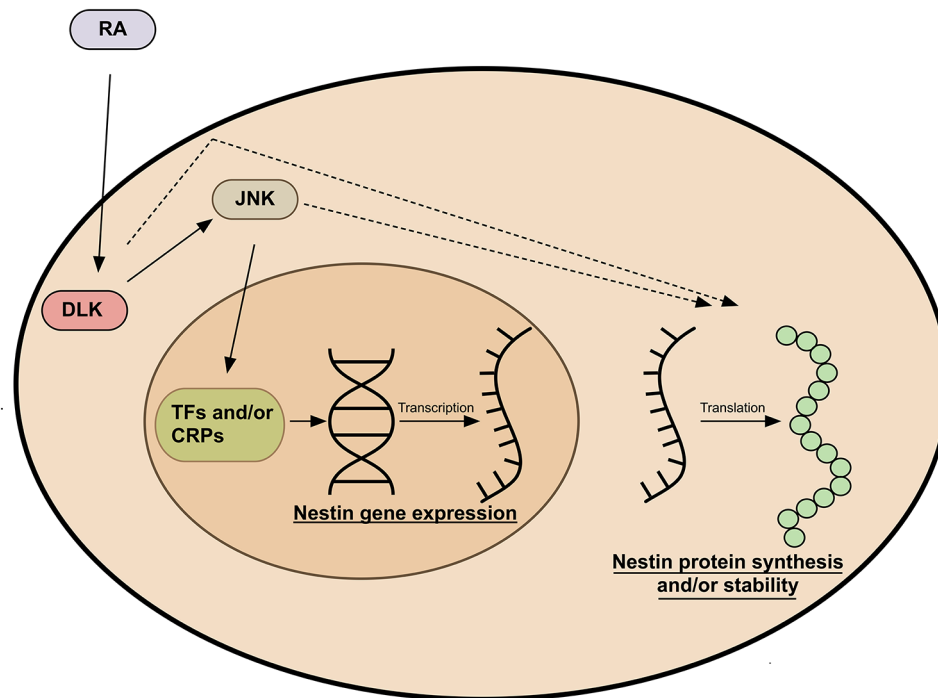


Fig. 6 Hypothetical model of DLK-mediated nestin regulation in RA-treated Neuro-2a cells. RA activates the DLK-JNK signaling pathway, which subsequently enhances nestin gene expression through the action of specific transcription factors (TFs) and/or chromatin regulatory proteins (CRPs). Alternatively, or in addition (as indicated by dotted arrows), DLK may contribute to nestin protein accumulation in RA-treated cells by promoting its synthesis and/or its stability

conditions. Interestingly, this response is not a direct consequence of the loss of nestin function in NSPCs but is caused by reduced Notch signaling between astrocytes and neural stem cells [70]. Notch signaling is known to promote proliferation during neurogenesis, whereas its inhibition induces neuronal differentiation both in vitro and in vivo [71]. Thus, nestin appears to antagonize the neuronal differentiation of neural stem cells through its ability to upregulate Notch signaling in astrocytes. In the present study, which used monocultures of Neuro-2a cells, a mouse neural crest-derived cell line capable of differentiating into neurons [72], we observed that RA simultaneously induces the upregulation of nestin levels and neurite outgrowth in a DLK-dependent manner. These effects of RA appeared to be independent of each other since neither knockdown nor overexpression of nestin in Neuro-2a cells caused detectable changes in RA-induced neurite formation and outgrowth (Figs. 4 and 5), which are the hallmarks of differentiated cells. Therefore, we concluded that nestin does not have an obvious direct role in regulating neurite extension in Neuro-2a cells. However, because neurite formation is a complex process involving cytoskeletal rearrangements, plasma membrane extension, second messenger production and postranslational modification [73, 74], we cannot exclude the possibility that nestin plays a role in the neuronal differentiation of Neuro-2a cells, which is too

subtle to be detected in our assays. Further studies will be needed to fully evaluate whether there is a link between DLK signaling, nestin expression and neurite outgrowth.

In addition to being expressed in NSPCs, nestin is also transiently expressed in the axons of newborn neurons, where it plays a role in growth cone morphology and the response to the axonal guidance cue semaphorin 3 A (Sema3A). Indeed, in the absence of nestin, neurons exhibit larger growth cones and reduced sensitivity to Sema3A [75], which induces growth cone collapse and axon repulsion in culture [76]. Mechanistically, the effect of nestin on growth cones and Sema3A sensitivity can be attributed, at least in part, to cdk5/p35-mediated phosphorylation of doublecortin (DCX) [77], a critical regulator of microtubule (MT) structure, stability and function in immature neurons [78, 79]. These findings are of particular importance because the DLK-JNK pathway has been reported to regulate (i) the expression of axon guidance proteins [21], such as neuropilin 1, which functions as a transmembrane cellular receptor for Sema3A, and (ii) axonogenesis via the phosphorylation of several MT regulators, including DCX [7, 16]. Therefore, through their ability to both modulate DCX phosphorylation, nestin and DLK are likely capable of regulating the microtubule cytoskeleton, whose organization and remodeling are essential for axonal growth and guidance as well as migration in developing neurons [80]. Thus, the

impact of DLK-mediated regulation of nestin expression on microtubule structure and dynamics during neuronal differentiation is an important question that needs to be addressed by further research.

Conclusion

Our study identifies for the first time a link between the regulation of nestin expression and DLK signaling in RA-exposed neuroblastoma Neuro-2a cells. The importance of nestin regulation by DLK for neuronal differentiation remains puzzling, especially because nestin knockdown or overexpression did not disrupt neurite outgrowth in these cells. Further work is needed to define the role of nestin in the organization and integrity of the neuronal cytoskeleton and to determine its contribution, if any, to DLK-mediated neurite outgrowth.

Abbreviations

BSA	Bovine serum albumin
CAM	Cell adhesion molecule
CNS	Central nervous system
CRPs	Chromatin regulatory proteins
DLK	Dual leucine zipper kinase
DMEM	Dulbecco's modified Eagle's medium
DRG	Dorsal root ganglion
ECL	Extracellular matrix
FBS	Fetal bovine serum
IF	Intermediate filament
iTRAQ	Isobaric tags for relative and absolute quantitation
JNK	c-Jun N-terminal kinase
PNS	Peripheral nervous system
PRM	Parallel reaction monitoring
RA	Retinoic acid
qRT-PCR	Real time quantitative reverse transcription PCR
TFs	Transcription factors

Supplementary Information

The online version contains supplementary material available at <https://doi.org/10.1186/s12860-025-00535-x>.

Supplementary Material 1: Raw data (uncropped western blots) for Fig. 1A.

Supplementary Material 2: Raw data (uncropped western blots) for Fig. 3B.

Supplementary Material 3: Raw data (uncropped western blots) for Fig. 4A.

Supplementary Material 4: Raw data (uncropped western blots) for Fig. 5A.

Supplementary Material 5: List of primary and secondary antibodies used in this study.

Supplementary Material 6: List of primers used for qPCR.

Acknowledgements

We thank Dr. Alain Lavigne for critical reading of the manuscript.

Author contributions

G.S.-C. and R.B. conceived the study, performed experiments, analyzed data and wrote the manuscript; D.G. and N.G. reviewed and edited the manuscript. All authors read and approved the final manuscript.

Funding

This research was supported by the Natural Sciences and Engineering Research Council of Canada (2017–05402).

Data availability

The datasets generated and analyzed during the current study are available from the corresponding author upon reasonable request.

Declarations

Ethics approval and consent to participate

Not applicable.

Consent for publication

Not applicable.

Competing interests

The authors declare no competing interests.

Received: 17 December 2024 / Accepted: 20 March 2025

Published online: 26 March 2025

References

1. Kamiguchi H. The role of cell adhesion molecules in axon growth and guidance. *Adv Exp Med Biol.* 2007;621:95–103.
2. Polleux F, Snider W. Initiating and growing an axon. *Cold Spring Harb Perspect Biol.* 2010;2:a001925.
3. Tedeschi A. Tuning the orchestra: transcriptional pathways controlling axon regeneration. *Front Mol Neurosci.* 2012;4:1–12.
4. Gallo KA, Johnson GL. Mixed-lineage kinase control of JNK and p38 MAPK pathways. *Nat Rev Mol Cell Biol.* 2002;3:663–72.
5. Coffey ET. Nuclear and cytosolic JNK signalling in neurons. *Nat Rev Neurosci.* 2014;15:285–99.
6. Jin Y, Zheng B, Multitasking. Dual leucine zipper-bearing kinases in neuronal development and stress management. *Annu Rev Cell Dev Biol.* 2019;35:501–21.
7. Hirai S, Cui DF, Miyata T, Ogawa M, Kiyonari H, Suda Y, et al. The c-Jun N-terminal kinase activator dual leucine zipper kinase regulates axon growth and neuronal migration in the developing cerebral cortex. *J Neurosci.* 2006;26:11992–2002.
8. Shin JE, Cho Y, Beirowski B, Milbrandt J, Cavalli V, DiAntonio A. Dual leucine zipper kinase is required for retrograde injury signaling and axonal regeneration. *Neuron.* 2012;74:1015–22.
9. Watkins TA, Wang B, Huntwork-Rodriguez S, Yang J, Jiang Z, Eastham-Anderson J, et al. DLK initiates a transcriptional program that couples apoptotic and regenerative responses to axonal injury. *Proc Natl Acad Sci U S A.* 2013;110:4039–44.
10. Hao Y, Frey E, Yoon C, Wong H, Nestorovski D, Holzman LB et al. An evolutionarily conserved mechanism for cAMP elicited axonal regeneration involves direct activation of the dual leucine zipper kinase DLK. *Elife.* 2016;5.
11. Miller BR, Press C, Daniels RW, Sasaki Y, Milbrandt J, DiAntonio A. A dual leucine kinase-dependent axon self-destruction program promotes wallerian degeneration. *Nat Neurosci.* 2009;12:387–9.
12. Pozniak CD, Sengupta Ghosh A, Gogineni A, Hanson JE, Lee S-H, Larson JL, et al. Dual leucine zipper kinase is required for excitotoxicity-induced neuronal degeneration. *J Exp Med.* 2013;210:2553–67.
13. Welsbie DSSDS, Yang Z, Ge Y, Mitchell KLKL, Zhou X, Martin SEESE, et al. Functional genomic screening identifies dual leucine zipper kinase as a key mediator of retinal ganglion cell death. *Proc Natl Acad Sci U S A.* 2013;110:4045–50.
14. Le Pichon CE, Meilandt WJ, Dominguez S, Solanoy H, Lin H, Ngu H, et al. Loss of dual leucine zipper kinase signaling is protective in animal models of neurodegenerative disease. *Sci Transl Med.* 2017;9:eaag0394.
15. Eto K, Kawachi T, Osawa M, Tabata H, Nakajima K. Role of dual leucine zipper-bearing kinase (DLK/MUK/ZPK) in axonal growth. *Neurosci Res.* 2010;66:37–45.
16. Gdalyahu A, Ghosh I, Levy T, Sapir T, Sapoznik S, Fishler Y, et al. DCX, a new mediator of the JNK pathway. *EMBO J.* 2004;23:823–32.
17. Dehmelt L, Smart FM, Ozer RS, Halpain S. The role of microtubule-associated protein 2c in the reorganization of microtubules and lamellipodia during neurite initiation. *J Neurosci.* 2003;23:9479–90.

18. Teng J, Takei Y, Harada A, Nakata T, Chen J, Hirokawa N. Synergistic effects of MAP2 and MAP1B knockout in neuronal migration, dendritic outgrowth, and microtubule organization. *J Cell Biol.* 2001;155:65–76.
19. Raivich G. c-Jun expression, activation and function in neural cell death, inflammation and repair. *J Neurochem.* 2008;107:898–906.
20. Bareyre FM, Garzorz N, Lang C, Misgeld T, Büning H, Kerschensteiner M. In vivo imaging reveals a phase-specific role of STAT3 during central and peripheral nervous system axon regeneration. *Proc Natl Acad Sci U S A.* 2011;108:6282–7.
21. Blondeau A, Lucier J-F, Matteau D, Dumont L, Rodrigue S, Jacques, et al. Dual leucine zipper kinase regulates expression of axon guidance genes in mouse neuronal cells. *Neural Dev.* 2016;11:13.
22. Lowery J, Kuczmarski ER, Herrmann H, Goldman RD. Intermediate filaments play a pivotal role in regulating cell architecture and function. *J Biol Chem.* 2015;290:17145–53.
23. Sharma P, Alsharif S, Fallatah A, Chung BM. Intermediate filaments as effectors of cancer development and metastasis: A focus on keratins, vimentin, and Nestin. *Cells.* 2019;8:497.
24. Stewart SA, Dykxhoorn DM, Palliser D, Mizuno H, Yu EY, An DS, et al. Lentivirus-delivered stable gene silencing by RNAi in primary cells. *RNA.* 2003;9:493–501.
25. Daviau A, Couture J-P, Blouin R. Loss of DLK expression in WI-38 human diploid fibroblasts induces a senescent-like proliferation arrest. *Biochem Biophys Res Commun.* 2011;413:282–7.
26. Choi S, Kelber J, Jiang X, Strnadl J, Fujimura K, Pasillas M et al. Procedures for the biochemical enrichment and proteomic analysis of the cytoskeleton. *Anal Biochem.* 2014;446.
27. Bourassa S, Fournier F, Nehmé B, Kelly I, Tremblay A, Lemelin V, et al. Evaluation of iTRAQ and SWATH-MS for the quantification of proteins associated with insulin resistance in human duodenal biopsy samples. *PLoS ONE.* 2015;10:e0125934.
28. Sheta R, Woo CM, Roux-Dalvai F, Fournier F, Bourassa S, Droit A, et al. A metabolic labeling approach for glycoproteomic analysis reveals altered glycoprotein expression upon GALNT3 knockdown in ovarian cancer cells. *J Proteom.* 2016;145:91–102.
29. Rauniyar N. Parallel reaction monitoring: A targeted experiment performed using high resolution and high mass accuracy mass spectrometry. *Int J Mol Sci.* 2015;16:28566–81.
30. Pino LK, Searle BC, Bollinger JG, Nunn B, Maclean B, Maccoss MJ. The skyline ecosystem: informatics for quantitative mass spectrometry proteomics. *Mass Spectrom Rev.* 2017. <https://doi.org/10.1002/mas.21540>.
31. Hellemans J, Mortier G, De Paeppe A, Speleman F, Vandesompele J. qBase relative quantification framework and software for management and automated analysis of real-time quantitative PCR data. *Genome Biol.* 2007;8:R19.
32. Brosseau J-P, Lucier J-F, Lapointe E, Durand M, Gendron D, Gervais-Bird J, et al. High-throughput quantification of splicing isoforms. *RNA.* 2010;16:442–9.
33. Hammarlund M, Nix P, Hauth L, Jorgensen EM, Bastiani M. Axon regeneration requires a conserved MAP kinase pathway. *Science.* 2009;323:802–6.
34. Angel P, Hattori K, Smeal T, Karin M. The Jun proto-oncogene is positively autoregulated by its product, Jun/AP-1. *Cell.* 1988;55:875–85.
35. Hirai SS-i, Banba Y, Satake T, Ohno S. Axon formation in neocortical neurons depends on Stage-Specific regulation of microtubule stability by the dual leucine zipper kinase-c-Jun N-Terminal kinase pathway. *J Neurosci.* 2011;31:6468–80.
36. Barnat M, Enslin H, Propst F, Davis RJ, Soares S, Nothias F. Distinct roles of c-Jun N-Terminal kinase isoforms in neurite initiation and elongation during axonal regeneration. *J Neurosci.* 2010;30:7804–16.
37. Danzi MC, Mehta ST, Dulla K, Zunino G, Cooper DJ, Bixby JL, et al. The effect of Jun dimerization on neurite outgrowth and motif binding. *Mol Cell Neurosci.* 2018;92:114–27.
38. Raivich G, Bohatschek M, Da Costa C, Iwata O, Galiano M, Hristova M, et al. The AP-1 transcription factor c-Jun is required for efficient axonal regeneration. *Neuron.* 2004;43:57–67.
39. Minden A, Lin A, Smeal T, Dérjard B, Cobb M, Davis R et al. c-Jun N-terminal phosphorylation correlates with activation of the JNK subgroup but not the ERK subgroup of mitogen-activated protein kinases. *Mol Cell Biol.* 1994;14.
40. Pollscheidt J, Glaubitz N, Haller H, Horstkorte R, Bork K. Phosphorylation of Serine 774 of the neural cell adhesion molecule is necessary for cyclic adenosine monophosphate response element binding protein activation and neurite outgrowth. *J Neurosci Res.* 2012;90:1577–82.
41. Wu X, Tian L, Li J, Zhang Y, Han V, Li Y, Molecular, et al. *Cell Proteom.* 2012;11:1640–51.
42. Namiki J, Suzuki S, Masuda T, Ishihama Y, Okano H. Nestin protein is phosphorylated in adult neural stem/progenitor cells and not endothelial progenitor cells. *Stem Cells Int.* 2012;2012:430138.
43. Contreras-Vallejos E, Utreras E, Bórquez DA, Prochazkova M, Terse A, Jaffe H, et al. Searching for novel Cdk5 substrates in brain by comparative phosphoproteomics of wild type and Cdk5^{-/-} mice. *PLoS ONE.* 2014;9:e90363.
44. Bernal A, Arranz L. Nestin-expressing progenitor cells: function, identity and therapeutic implications. *Cell Mol Life Sci.* 2018;75:2177–95.
45. Xiong X, Wang X, Ewanek R, Bhat P, DiAntonio A, Collins CA. Protein turnover of the Wallenda/DLK kinase regulates a retrograde response to axonal injury. *J Cell Biol.* 2010;191:211–23.
46. Gilyarov AV. Nestin in central nervous system cells. *Neurosci Behav Physiol.* 2008;38:165–9.
47. Hockfield S, McKay RD. Identification of major cell classes in the developing mammalian nervous system. *J Neurosci.* 1985;5:3310–28.
48. Dahlstrand J, Zimmerman LB, McKay RD, Lendahl U. Characterization of the human Nestin gene reveals a close evolutionary relationship to neurofilaments. *J Cell Sci.* 1992;103.
49. Zimmerman L, Lendahl U, Cunningham M, McKay R, Parr B, Gavin B, et al. Independent regulatory elements in the Nestin gene direct transgene expression to neural stem cells or muscle precursors. *Neuron.* 1994;12:11–24.
50. Cheng L, Jin Z, Liu L, Yan Y, Li T, Zhu X et al. Characterization and promoter analysis of the mouse Nestin gene. *FEBS Lett.* 2004;565.
51. Jin Z, Liu L, Bian W, Chen Y, Xu G, Cheng L et al. Different transcription factors regulate Nestin gene expression during P19 cell neural differentiation and central nervous system development. *J Biol Chem.* 2009;284.
52. Stevanovic M, Drakulic D, Lazic A, Ninkovic DS, Schwirtlich M, Mojsin M. SOX transcription factors as important regulators of neuronal and glial differentiation during nervous system development and adult neurogenesis. *Front Mol Neurosci.* 2021;14.
53. Dong WH, Do JT, Araúzo-Bravo MJ, Sung HL, Meissner A, Hoon TL et al. Epigenetic hierarchy governing Nestin expression. *Stem Cells.* 2009;27.
54. Zhang J, Gao Y, Yu M, Wu H, Ai Z, Wu Y et al. Retinoic acid induces embryonic stem cell differentiation by altering both encoding RNA and MicroRNA expression. *PLoS ONE.* 2015;10.
55. Yu S, Levi L, Siegel R, Noy N. Retinoic acid induces neurogenesis by activating both retinoic acid receptors (RARs) and peroxisome proliferator-activated receptor B/δ (PPARβ/δ). *J Biol Chem.* 2012;287.
56. Janesick A, Wu SC, Blumberg B. Retinoic acid signaling and neuronal differentiation. *Cell Mol Life Sci.* 2015;72.
57. Khatib T, Marini P, Nunna S, Chisholm DR, Whiting A, Redfern C et al. Genomic and non-genomic pathways are both crucial for peak induction of neurite outgrowth by retinoids. *Cell Communication Signal.* 2019;17.
58. Al Tanoury Z, Piskunov A, Rochette-Egly C. Vitamin A and retinoid signaling: genomic and nongenomic effects. *J Lipid Res.* 2013;54.
59. Tiwari VK, Stadler MB, Wirbelauer C, Paro R, Schübeler D, Beisel C. A chromatin-modifying function of JNK during stem cell differentiation. *Nat Genet.* 2012;44:94–100.
60. Devaiah BN, Singh AK, Mu J, Chen Q, Meerzaman D, Singer DS. Phosphorylation by JNK switches BRD4 functions. *Mol Cell.* 2024;84:4282–e42967.
61. Kasibhatla S, Tailor P, Bonefoy-Berard N, Mustelin T, Altman A, Fotedar A. Jun kinase phosphorylates and regulates the DNA binding activity of an octamer binding protein, T-Cell factor B1. *Mol Cell Biol.* 1999;19.
62. Bae KB, Yu DH, Lee KY, Yao K, Ryu J, Lim DY, et al. Serine 347 phosphorylation by JNKs negatively regulates OCT4 protein stability in mouse embryonic stem cells. *Stem Cell Rep.* 2017;9:2050–64.
63. Bogoyevitch MA, Kobe B. Uses for JNK: the many and varied substrates of the c-Jun N-Terminal kinases. *Microbiol Mol Biol Rev.* 2006;70.
64. Huang X-Q, Huang Z-X, Li Z-L, Chen X-W, Li X, Tang X-C et al. C-Jun terminal kinases play an important role in regulating embryonic survival and eye development in vertebrates. *Curr Mol Med.* 2012;13.
65. Singh M, Ye B, Kim JH. Dual leucine zipper kinase regulates Dscam expression through a noncanonical function of the cytoplasmic Poly(A)-Binding protein. *J Neurosci.* 2022;42.
66. Sabapathy K, Hochedlinger K, Nam SY, Bauer A, Karin M, Wagner EF. Distinct roles for JNK1 and JNK2 in regulating JNK activity and c-Jun-dependent cell proliferation. *Mol Cell.* 2004;15.
67. Jaeschke A, Karasirides M, Ventura JJ, Ehrhardt A, Zhang C, Flavell RA et al. JNK2 is a positive regulator of the cJun transcription factor. *Mol Cell.* 2006;23.
68. Lothian C, Lendahl U. An evolutionary conserved region in the second intron of the human Nestin gene directs gene expression to CNS progenitor cells and to early neural crest cells. *Eur J Neurosci.* 1997;9.

69. Mohseni P, Sung HK, Murphy AJ, Laliberte CL, Pallari HM, Henkelman M et al. Nestin is not essential for development of the CNS but required for dispersion of acetylcholine receptor clusters at the area of neuromuscular junctions. *J Neurosci*. 2011;31.
70. Wilhelmsson U, Lebkuechner I, Leke R, Marasek P, Yang X, Antfolk D et al. Nestin regulates neurogenesis in mice through Notch signaling from astrocytes to neural stem cells. *Cereb Cortex*. 2019;29.
71. Lampada A, Taylor V. Notch signaling as a master regulator of adult neurogenesis. *Front NeuroSci*. 2023;17.
72. Tremblay RG, Sikorska M, Sandhu JK, Lanthier P, Ribocco-Lutkiewicz M, Bani-Yaghoub M. Differentiation of mouse neuro 2A cells into dopamine neurons. *J Neurosci Methods*. 2010;186:60–7.
73. Lewis TL, Courchet J, Polleux F. Cellular and molecular mechanisms underlying axon formation, growth, and branching. *J Cell Biol*. 2013;202.
74. Sainath R, Gallo G. Cytoskeletal and signaling mechanisms of neurite formation. *Cell Tissue Res*. 2014;359.
75. Bott CJ, Johnson CG, Yap CC, Dwyer ND, Litwa KA, Winckler B. Nestin in immature embryonic neurons affects axon growth cone morphology and Semaphorin3a sensitivity. *Mol Biol Cell*. 2019;30:1214–29.
76. Tang B. Semaphorin 3A: from growth cone repellent to promoter of neuronal regeneration. *Neural Regen Res*. 2018;13:795.
77. Bott CJ, McMahon LP, Keil JM, Choo Yap C, Kwan KY, Winckler B. Nestin selectively facilitates the phosphorylation of the Lissencephaly-Linked protein doublecortin (DCX) by cdk5/p35 to regulate growth cone morphology and Sema3a sensitivity in developing neurons. *J Neurosci*. 2020;40.
78. Francis F, Koulakoff A, Boucher D, Chafey P, Schaar B, Vinet MC et al. Doublecortin is a developmentally regulated, microtubule-associated protein expressed in migrating and differentiating neurons. *Neuron*. 1999;23.
79. Moores CA, Perderiset M, Francis F, Chelly J, Houdusse A, Milligan RA. Mechanism of microtubule stabilization by doublecortin. *Mol Cell*. 2004;14.
80. Atkins M, Nicol X, Fassier C. Microtubule remodelling as a driving force of axon guidance and pruning. *Seminars Cell Dev Biology*. 2023;140.

Publisher's note

Springer Nature remains neutral with regard to jurisdictional claims in published maps and institutional affiliations.